Multi-objective optimization to improve the performance of Delta Robot for a predefined workspace

Yussuf Reza Esmaeili, * Hamed Moradi, Gholamreza Vossoughi
School of Mechanical Engineering, Sharif University of Technology, Tehran, Iran, Tel: (+98) 21-66165545, Fax: (+98) 21-66000021

* *hamedmoradi@sharif.edu*

Abstract

Due to conflictions between different purposes and objectives of the industrial robots, a multi-objective optimization is required to find the non-dominant answers to choose from. In this article, we have introduced a new optimization objective which involves the robot's high acceleration, actuator effort reduction; while avoiding the singularities which is applicable on any robot with an approximate known inverse dynamic. The cost function is defined by designing a computed torque control on robot. Our objectives are defined as: 1. minimizing the root mean square (RMS) power needed in motors for movements with the maximum acceleration of the end effector in different directions (cost/effort reduction), 2. Minimizing the mean Jacobian condition number in a predefined workspace (kinematic performance improvement) and 3. Minimizing the mass matrix condition number in a predefined workspace (dynamic performance improvement). The multi-objective problem is numerically solved using a genetic algorithm, yielding non-dominated solutions known as Pareto fronts. Geometrical design variables are chosen from Pareto fronts by three different Multiple-Criteria Decision Making (MCDM) methods. Eventually, cost functions of the designed robot are compared with a Fanuc M-2iA/3S model.

Keywords: Delta Rotary Robot, Parallel Robot, Multi-Objective Optimization, Genetic Algorithm, Multi-criteria Decision Making.

1. Introduction

The standard type of Delta parallel Robot which has 3 rotary actuators connected to 3 legs and parallelograms, was invented by Clavel in 1987 [1, 2]. Utilizing the actuators on top base, provides the robot with a light end effector, which results in high speeds and mobility. Different industrial and academic versions of Delta robot have been designed, optimized and manufactured [3-5]. In 2002, Bruzzone et al. designed and controlled a linear Delta robot which was for peg-in-hole problem. They utilized the equivalent mechanisms rather than parallelograms [6]. In 1998, Tsumaki et al. designed a compact 6 DOF haptic interface with a large workspace [7]. It contained a five-bar spatial mechanism for orientation which is positioned on a Delta Mechanism that allows high speeds due to parallel mechanism. In 2021, Meza et al. designed and kinematically analyzed a delta robot for a predefined workspace on supermarkets for social distancing during Covid-Pandemic [8].

Some research focused on Robot's workspace mainly with the objective of maximizing the workspace and avoiding the singularities [9-13]. Laribi et al. solved the problem of finding suitable design variables of a Delta robot in order to have the nearest real workspace to a desired workspace shape and size [14]. Some researchers used computer assisted design for determining and optimizing joint areas reached by arms[12, 13]. In 2019, McCormick optimized the objective of minimum unutilized workspace of the rotary Delta robot by two methods of genetic algorithm and maximum surrounding workspace[15].

There are other optimizations focused on the stiffness of the robot allowing high positioning accuracy[16]. In 2020, by considering the compliance matrix for stiffness formulation, Mirz performed an optimization on the Delta robot using genetic algorithm[17].

In 2003, Stock and Miller optimized a kinematic design on linear Delta robot and examined the mobility, workspace and manipulability and concluded that manipulability and workspace are contradictory, since solely optimizing the manipulability leads to a zero workspace [18]. Therefore, solely optimizing one objective may result in robot's failure and simultaneously considering different objectives is required. In 2004, Miller optimized and modeled the Delta parallel manipulator by considering two objectives of maximizing workspace volume and manipulability [19]. In 2012, Kelaiaia et al. performed a multi-objective optimization on a linear Delta parallel robot [20]. Their optimization criteria were workspace, stiffness, kinematic and dynamic performances, and they solved the multi-objective problem by defining constraints and application of genetic algorithm SPEA-II. He used the Jacobian condition number for measuring the manipulability as well as Kelaiaia in [20]. In 2016, Bounab solved a multi-objective optimal design problem for Delta mechanism and its criteria was to find the maximum regular workspace where the robot must possess the maximum stiffness and dexterity [21]. In that work, Castigliano's energetic theorem was used for modeling the elastostatic behavior of Delta robot and numerically solved the problem with genetic algorithm [21]. In 2021, Yang et al. considered two conflicting objectives of lightweight and high stiffness and used sensitivity analysis and response surface methods for optimization [22]. In 2021, Ohno et al. defined joint impact index to evaluate the magnitude of actuation torque fluctuation due to the collision at the passive joints with clearances and solved its target trajectories using multi-objective optimization [23].

In 2021, Carabin et al. proposed using elastic elements such as springs to increase Delta robot's energy efficiency [24]. Although so many optimizations have been done on Delta robot, none of the previous works consider cost reduction and minimizing the actuator effort by considering arm length. In this paper, a new optimization goal has been introduced which is to reduce the actuator effort by considering both Delta robot's high acceleration, and the manipulator's ability to follow desired paths in workspace. An approximation of the robot's inverse dynamics is mandatory to define the cost function[25, 26]. Hence, we use the Codourey et al. dynamic modeling which is based on the virtual work principle [27-29]. We will use Laribi's and Staicu's inverse kinematics equations for our constraints [14, 30, 31]. There are state-of-the-art adaptive robust iterative control [32] and backstepping [33] control of Delta robot but to analyze the optimization results, a multi-layer sliding mode control method is designed on the robot. Control results demand the direct dynamics of the robot which is brought by [34, 35]. Since the exact direct dynamics of Delta robot is complicated, we will use Simulink to model and analyze the system.

We have also considered two other objectives of kinematics and dynamics performance optimizations by utilizing the Jacobian and mass matrix condition number. Objectives are separately and simultaneously optimized, and Pareto optimal fronts are resulted. In the end, the multi-criteria decision making (MCDM) problem of choosing the answer from the Pareto front is solved. Initially, the weights of each criterion is determined using Entropy method and by using these weight and utilization of three different methods of CODAS, PROMETHEE II and ELECTRE, the best geometrical specifications are chosen and compared with the Fanuc industrial Delta robot [36].

2. Kinematics of Delta Robot

Solution of kinematics of the robot is necessary for solving its inverse dynamics. The inverse dynamics of the robot is the key for analysis of the first objective Equation 1 is the relation between the input angular speeds ($\dot{q} = \begin{bmatrix} \dot{q}_1 & \dot{q}_2 & \dot{q}_3 \end{bmatrix}^T$) and output speed of the end effector ($\dot{X} = \begin{bmatrix} \dot{x} & \dot{y} & \dot{z} \end{bmatrix}^T$). J is known as the Jacobian matrix.

$$\dot{X} = J\dot{q} \tag{1}$$

Conforming Figure 1, from the output position, we mean the location of the end effector center (point P), and from the input angle *"i" (i=1,2,3),* we mean the angle of motor no. "*i*" with the horizontal plane (XY). Jacobian matrix is defined as below [37]:

$$J = -\begin{bmatrix} S_1^T \\ S_2^T \\ S_3^T \end{bmatrix}^{-1} \begin{pmatrix} S_1^T b_1 & 0 & 0 \\ 0 & S_2^T b_2 & 0 \\ 0 & 0 & S_3^T b_3 \end{pmatrix} \tag{2}$$

in which,

$$S_i = \begin{bmatrix} x \\ y \\ z \end{bmatrix} - {}^R_i R \left(\begin{bmatrix} R \\ 0 \\ 0 \end{bmatrix} + \begin{bmatrix} L_1 \cos q_i \\ 0 \\ L_1 \sin q_i \end{bmatrix} \right) \qquad \text{for} \quad i = 1,2,3 \tag{3}$$

$$b_i = \begin{bmatrix} L_1 \sin q_i \\ 0 \\ -L_1 \cos q_i \end{bmatrix} \qquad \text{for} \quad i = 1,2,3 \tag{4}$$

where, $R = R_a - R_b$.

Rotational matrix ${}^R_i R$ is defined by Eq. (5), in which θ_i is the rotation angle of the motors in the XY plane which is constant; while $\begin{bmatrix} \theta_1 & \theta_2 & \theta_3 \end{bmatrix} = 0, \pm 120^\circ$

$${}^R_i R = \begin{pmatrix} \cos\theta_i & -\sin\theta_i & 0 \\ \sin\theta_i & \cos\theta_i & 0 \\ 0 & 0 & 1 \end{pmatrix} \tag{5}$$

Equation (6) will be resulted by differentiating from Eq. (1) as:

$$\ddot{X} = -\begin{bmatrix} S_1^T \\ S_2^T \\ S_3^T \end{bmatrix}^{-1} \left(\begin{bmatrix} \dot{S}_1^T \\ \dot{S}_2^T \\ \dot{S}_3^T \end{bmatrix} J + K \right) \dot{q} + J\ddot{q} \tag{6}$$

In which, $K = \begin{pmatrix} \dot{S}_1^T b_1 + S_1^T \dot{b}_1 & 0 & 0 \\ 0 & \dot{S}_2^T b_2 + S_2^T \dot{b}_2 & 0 \\ 0 & 0 & \dot{S}_3^T b_3 + S_3^T \dot{b}_3 \end{pmatrix}$, $\dot{S}_i = \dot{X} + b_i \dot{q}_i$ and $\dot{b}_i = {}^R_i R \begin{bmatrix} L_1 \cos q_i \\ 0 \\ L_1 \sin q_i \end{bmatrix} \dot{q}_i$

for $i = 1,2,3$.

Jacobian matrix given by Eq. (2) is useless at the current form and it is not practical, since it contains the terms from the input and output simultaneously. Hence, the robot geometry should be solved. We will use the Laribi's inverse geometry solution [14] as:

$$l_i \cos q_i + m_i \sin q_i - n_j = 0 \tag{7}$$

In which:

$l_i = 2\left(R \cdot L_1 - L_1 x \cos\theta_i - L_1 y \sin\theta_i\right)$, $m_i = 2L_1 z$ and $n_i = -2Rx\cos\theta_i - 2Ry\sin\theta_i + x^2 + y^2 + z^2 + R^2 + L_1^2 - L_2^2$.

Inverse geometry means that with having the end effector's output position, we obtain the input angles. Equation (7), has two solutions as Eq. (8) and the correct answer will have the positive sign (+) before the radical.

$$\sin q_i = \frac{m_i n_i \pm \sqrt{m_i^{\,2} + l_i^{\,2} - n_i^{\,2}}}{m_i^{\,2} + l_i^{\,2}} \tag{8}$$

2.1 Supplementary angle condition: Inverse geometry's solution leads to the sinus of angles. Using the arc sinus function for obtaining the angle's amount eventuates an issue. For $\sin(q) = \alpha$, both $q = \arcsin\alpha$ and $q = \pi - \arcsin\alpha$ are correct. In most locations of the robot's workspace, input angles are acute, but in some locations specially, far from the origin, angles are more than 90°. We need to distinguish between these solutions and find the correct answer in order to correctly compute the fitness functions for optimization.

According to Figure 2, the correct angle is the one which leads to the length of *BC* to be equal to *L2* (length of the parallelogram). This condition must be applied to the solution.

3. Dynamics of Rotary Delta Robot

In dynamics of the Delta robot, motor torques are the inputs and the end effector's acceleration is the output. The inverse dynamics solution of the robot is mandatory for definition and measurement of the objectives, so that for a known and desired end effector's movement, input torques are computed. This is also known as computed torque control which is a predictive functional method [38].

Delta robot has a nonlinear, complex and coupled dynamics and attributing a torque to a single motor, will affect the other motors. Applying the incorrect torque to a motor will result in high tracking errors or even damage and breakdown. Precise dynamics of the Delta robot is not available and only approximate dynamics can be used.

The Codoury's model [27-29] has been used for inverse dynamics. Codoury has used the virtual work method for inverse dynamics' solution. For simplification, rather than considering the parallelogram's big side's mass as continuous, it is distributed into two-point masses at side's endings as shown in Figure 3.

with mass distribution's approximation, inverse dynamics problem is solved as [28]:

$$\tau = \psi p \tag{9}$$

where

$$\psi = \begin{bmatrix} g_1 & \ddot{q}_1 & 0 & 0 & 0 & 0 & \\ 0 & 0 & g_2 & \ddot{q}_2 & 0 & 0 & J^T\left(\ddot{X} - G\right) \\ 0 & 0 & 0 & 0 & g_3 & \ddot{q}_3 & \end{bmatrix}$$

$$p = \left[m_1 r_{1,x}, I_{1,yy}, m_2 r_{2,x}, I_{2,yy}, m_3 r_{3,x}, I_{3,yy}, m_n \right]^T$$

in which, $g_i = g \cos q_i$ and $G = \begin{bmatrix} 0 & 0 & g \end{bmatrix}^T$, and for masses,

$$m_i = m_{l1} + \frac{2}{3} m_{l2} + m_{l3},$$

$$m_n = m_t + 3 \times \left(\frac{1}{3} m_{l2} + m_{l3} \right) = m_t + m_{l2} + 3 m_{l3} \text{ for } i = 1, 2, 3.$$

In the formulas, m_{l1} represents first elbow's mass, m_{l2} the parallelogram's big side's mass, g the gravity, m_t the payload, and m_{l3} the parallelograms' small side's mass.

Additionally, $r_{i,x}$ is the distance between i^{th} elbow from the motor and $I_{i,yy}$ is the second momentum inertia of i^{th} elbow with respect to i^{th} motor.

Inverse dynamics' standard form equation is resulted by rewriting the equation solely with linear acceleration as:

$$\tau = \xi \ddot{X} + \delta \tag{10}$$

in which:

$$\xi = \begin{bmatrix} \frac{S_1^T}{S_1^T b_1} & \frac{S_2^T}{S_2^T b_2} & \frac{S_3^T}{S_3^T b_3} \end{bmatrix}^T \times I_{i,yy} + m_n J^T$$

$$\delta = g m_i r_{i,x} \begin{bmatrix} \cos q_1 \\ \cos q_2 \\ \cos q_3 \end{bmatrix} + B \times I_{i,yy} g \times \left(J(3,:) \right)^T$$

3.1 Approximated Dynamics Error

To control the robot, error of the simplified dynamics must be approximated. Hence, for a sinusoidal movement with an amplitude of 15 cm (Figure 4), motor torques are computed by Eq. (10). Then, computed torques are applied to the motors and the end effector position is measured with Simulink. Then, this measured position is compared with the primitive desired position and error is measured.

Simplified dynamics error is shown in Figure 5. Note that there are no other errors or uncertainties other than dynamics. Error is $\pm 1mm$ in *X* and *Y* directions and $\pm 4mm$ in *Z* direction. Due to gravity, end effector's position is always lower than desired.

Properties of the system are as below:

```
l1=0.571 m    ,    l2=0.847 m
R=0.114 m     ,    h=0.32 m
ml1=0.634 Kg  ,    ml2=0.551 Kg
ml3=0.028 Kg  ,    mt=3.0 Kg
```

As the ratio of the end effector mass to the second elbow's mass (*mt/ml2*) decreases, simplified dynamics error increases, since the effect of mass distribution has a more impact on the system.

4. Objectives and Optimization Process

Pre-determined workspace of the Delta Robot is a cube with the side of b ($b=60\ cm$) and a height of h from the base, as shown in Figure 6. Design variables are including the: 1- first elbow length ($L1$), 2- Second elbow length ($L2$), 3- R and 4-h.

4.1 Constraints of the Problem

Constraints of the problem are listed as follows:

a) Motor torques should not go beyond a limit (motor constraint). We consider this limit as *45 N.m* with respect to a suitable industrial motor [39]. $\tau_{max} < \tau_{all}$

b) For each point in the workspace, a possible solution should exist for inverse geometry.

c) Due to the geometry limits, elbow lengths, R and height should be chosen from these intervals:
0 < h < 0.5 (m), 0 < R < 0.4 (m), 0.3 < L1 , L2 < 1 (m)

4.2 Objectives of the Problem

In this research, three objectives are considered:

Objective 1: Minimizing the root-mean-square (RMS) power needed in motors for the maximum acceleration movement of the end effector

High speed and agility are the features of Delta robot. At this problem, robot must perform point to point movements in the fastest time possible. If the highest acceleration would be assigned as "g", then the fastest way of a point-to-point travel is to start accelerating with "$+g$" from the start point to the path's midpoint and then decelerating with "$-g$" and finally stop at destination. This is called a bang-bang path, as shown in Figure 7.

Optimization should not tend to a specific path or direction and chosen paths should be distributed in all directions. The assigned paths contain the start point of cubic workspace's center and end point of workspace's boundary in different directions. In sum, 26 paths are chosen, RMS power is computed in each path and finally the average of these 26 paths is reported as the objective 1 fitness function value; as below:

Start point: $O(0,0,h+b/2)$

End point: $A_i(x_{end}, y_{end}, z_{end})$

$$X_{end}, Y_{end} \in \left\{-\frac{b}{2}, 0, +\frac{b}{2}\right\}, Z_{end} \in \left\{h, h+\frac{b}{2}, h+b\right\}$$

and $\left[X_{end}, Y_{end}, Z_{end}\right] \neq \left[0,0,h+\frac{b}{2}\right]$

$$\text{Obj 1: minimize } \frac{1}{26}\sum_{i=1}^{26} P_{rms}(\overline{OA_i}) \tag{11}$$

Objective 2: Improvement of the kinematic performance

A good kinematic performance, means that in all points of the workspace, the end effector could be able to move in all directions. In other words, moving in one direction shouldn't be harder than other directions which is defined as dexterity. As if the robot is kinematically isotropic and

dexterous. In order to define this as a cost function, we utilize the concept of condition number described in [20, 21].

Condition number of a matrix, calculates the ratio of its maximum singular value to minimum one. A matrix with determinant of zero, has an infinite condition number. Conversely, a completely isotropic matrix has a condition number of 1.

For a good kinematic performance of the robot in a specific position, its Jacobian condition number should tend to 1. Thus, minimizing the condition number of the Jacobian matrix (equal to 1 in the best case) for all points of the workspace, would be defined as the objective. Since, there are infinite points in the workspace, the average of a finite number of points must be calculated. For a uniform distribution of the workspace, we attribute 5 points with equal spacing to the cubic workspace on each axis (*X*,*Y*,*Z*), and a total of 125 distributed points in the workspace will be surveyed. The cost function of the objective 2 is defined as:

$$\text{Obj 2: minimize: } \frac{1}{N}\sum condition\_number(J) \tag{12}$$

In which N is equal to 125.

Objective 3: Improvement of the dynamic performance

In the previous objective, nothing about the inertia or mass was considered. Objective 3 is defined with an approach of accelerating in all directions, in which the mass and inertia are considered. Mass matrix is calculated as below [20]:

$$\tau = I(q)\ddot{q} + V(q,\dot{q})\dot{q} + G(q) \tag{13}$$

$$M = J^{-T} I(q) J^{-1} \tag{14}$$

and objective 3 is defined as:

$$\text{Obj 2: minimize: } \frac{1}{N}\sum condition\_number(M) \tag{15}$$

This objective means in a distributed point cloud (as defined in the previous objective), accelerating in all directions would be easy and uniformed and the robot is dynamically isotropic.

4.3 Optimization results

Objectives are separately optimized with genetic algorithm method and results are shown in Table 1.

Note that the results in Table 1, are the best possible values for each objective. Focusing on one objective may result in poor values in other objectives.

Figure 8 represents the optimization results and Pareto fronts for the Two-objective problem. There are three Pareto fronts for each two objectives, together.

The third Pareto front in Figure 8 concludes objectives 2 and 3 are consistent with each other due to a little change in their fitness function value.

Finally, three-objective optimization is solved, and Pareto surface is shown in Figure 9. Corresponding results are shown in Table 2.

5. Solving the MCDM problem of choosing the alternative

There is a total of six alternatives based on Table 2. These alternatives are resulted from the Pareto front; meaning they are dominant compared to all other designs. In this part, the best alternative is chosen with the help of three MCDM methods.

5.1 Calculating the normalized decision matrix

To make the comparison of these alternatives possible, the normalized decision matrix must be derived. To convert the minimization problem to maximization, inversion of each value can be done. Since lower values in all criteria of RMS power, Jacobian and mass condition number are favorable, all of values must be inversed after the normalization. The normalized decision matrix is derived as Table 3:

The next step of decision-making progress is determining the weights of each criterion.

5.2 Determining the weights of each criterion

There are different methods for determination of weights for each criterion such as direct weighting, Entropy method, Eigenvector method and SWARA method. In the direct weighting method, the expert determines the importance of each criterion. However, a more systematic method of determining the weights is the Entropy method. This method does not solely rely on expert's opinion and it uses the available information from the input data. the importance of each objective is determined through its variance among the alternatives. The walkthrough of Entropy method is brought in the following.

Step 1: Calculation of feature weight Pij for the i^{th} alternative and j^{th} criterion:

$$p_{ij} = \frac{a_{ij}}{\sum_{i=1}^{6} a_{ij}}, \quad 1 \le i \le 6 \quad , \quad 1 \le j \le 3 \tag{16}$$

Step 2: The output entropy e_j of the j^{th} factor is calculated as follows:

$$e_j = -\frac{1}{\ln 6} \sum_{i=1}^{6} p_{ij} \ln p_{ij} \quad , \quad 1 \le j \le 3 \tag{17}$$

Step 3: Calculation of weight of the entropy w_j:

$$w_j = \frac{1 - e_j}{\sum_{j=1}^{5} (1 - e_j)} \tag{18}$$

Using entropy method, the weights for each objective are derived which are 0.414, 0.0080 and 0.506 for criteria one to three, respectively.

5.3 MCDM methods for determining the best alternative

With weight coefficients for each criterion determined, MCDM method can be used.

1- CODAS (Combinative Distance-based Assessment) method

This method uses Euclidean and Texicab distances from the minimum value in each criterion and the assessment score is calculated afterwards. Table 4 shows the rankings of each alternative.

2- PROMETHEE II (preference ranking organization method for enrichment evaluation)

PROMETHEE II (complete ranking) method was developed by J.P. Brans [40]. This method consists in a preference function associated to each criterion as well as weights describing their relative importance. PROMETHEE II method is based on pairwise evaluation considering the difference (deviation) between two alternatives. The scores and rankings are represented in Table 5.

3- ELECTRE (Elimination Et Choice Translating Reality) method

The ELECTRE method helps with solving the concept of outranking relations encountered with diverse concrete problems [41]. In this method, the alternative with a higher concordance and lower discordance outranks other alternatives. The score of each alternative can be calculated with these values. The scores and rankings are shown in Table 6.

Even though all of the MCDM methods do not agree on all rankings, they mutually highlight fifth alternative (A5) as the first rank.

Pareto front resulted from objectives two and three has no vision on reducing the robot's size and two first design variables of *L1* and *L2* tend to upper limit. Hence, by surveying the Pareto optimal fronts, we choose:

L1=0.609 m, L2=0.843 m, R=0.094 m, h= 0.349 m

Fitness functions of this solution are shown in Table 7. By comparing the fitness functions with the optimization results of the three-objectives problem shown in Table 2, we find it is rather a good chosen answer by considering all goals altogether.

5.4 Comparison of the results with an industrial robot

Designed robot is compared with the well-known Fanuc industrial robot model M-2iA/3S [36] which is similar in payload (3 kg) and workspace dimensions to our designed robot. The comparison results are shown in Table 7. Although the workspace of the industrial robot is not an exact predefined cube, clearly, the proposed designed robot is better in fitness functions in almost every criterion.

6. Conclusion

A Delta robot is designed and optimized with objectives including the 1. Minimizing mean RMS power for bang-bang movements with an acceleration of gravity, 2. Improvement in kinematic and 3. Improvement in dynamic performance and making the robot isotropic for accelerating and movement. As most multi-objective optimizations, these objectives are inconsistent and conflicting. Therefore, by utilizing the genetic algorithm and extracting the Pareto optimal fronts, all non-dominant answers are discovered.

The multi-criteria decision making of choosing the final design among the Pareto front alternatives was executed in two stages. Initially, the weight factors of each criterion were calculated with Entropy method. Then, the MCDM problem was solved with three different state-of-the-art methods. All the methods mutually converged on one alternative and the design variables of the robot was determined.

The designed robot was compared with an industrial robot of Fanuc. Cost reduction, less movement power and torques, avoiding the kinematic and dynamic singularities in the predefined cubic workspace, better kinematic and dynamic performance and a better isotropy are our robot's improvements. However, industrial robot has smaller dimensions and as a result, gravity has less effect (lower static torques) and its workspace is more similar to the desired workspace.

Indeed, Delta robot still establishes rooms for improvement and further research. Delta robot's mechanism can be modified for a workspace with a large height. Although linear Delta mechanism is designed for these applications, it lacks the high operational speeds. Hence, a new modified mechanism can be beneficial. Also, adding the balance masses to the arms can reduces the gravity effects on the motor torques which increases the motors' durability and can increase the performance speed.

Conflict of Interest

None declared.

Data Availability

Data will be made available on reasonable request.

References

[1] Clavel R., "Delta, a fast robot with parallel geometry," *18th International Symposium on Industrial Robots,* pp. 91-100, 1988, https://doi.org/10.1007/978-1-4471-0885-6_29 .

[2] Clavel R., "Conception d'un robot parallèle rapide à 4 degrés de liberté," *Conception D'un Robot Parallèle Rapide à 4 Degrés de Liberté,* 1991, thesis.

[3] Bonev I., "Delta parallel robot - The story of success," *Delta parallel robot - The story of success,* 2001.

[4] Huang T., Li Z., Li M., et al. , "Conceptual design and dimensional synthesis of a novel 2-DOF translational parallel robot for pick-and-place operations," *Journal of Mechanical Design, Transactions of the ASME,* vol. 126, pp. 449-455, 2004, https://doi.org/10.1115/1.1711822.

[5] Laurin D., Lee B., Muff C., et al. , "Delta robot review article," Columbia university 2014.

[6] L. Bruzzone, R. Molfino, and M. Zoppi, "Modelling and control of peg-in-hole assembly performed by a translational robot," in *Proceedings of the International Conference Modeling Identification and Control, Austria*, 2002, pp. 512-7 https://doi.org/10.1108/aa-10-2018-0164 .

[7] Tsumaki Y., Naruse H., Nenchev D. N., et al. , "Design of a compact 6-DOF haptic interface," in *Robotics and Automation, 1998. Proceedings. 1998 IEEE International Conference on*, 1998, pp. 2580-2585, https://doi.org/10.1109/robot.1998.680730 .

[8] Meza B.H., Fernandez H.J., Cornejo J., et al. , 2021, October. Mechatronic design and kinematic analysis of Delta robot applied on supermarkets for social distancing during COVID-19 pandemic. In 2021 IEEE Engineering International Research Conference (EIRCON) (pp. 1-4). IEEE., 2021 https://doi.org/10.1109/eircon52903.2021.9613165]

[9] Gallant M. and Boudreau R., "The synthesis of planar parallel manipulators with prismatic joints for an optimal, singularity-free workspace," *Journal of Robotic Systems,* vol. 19, pp. 13-24, 2002.

[10] Stamper R. E., Tsai L.-W., and Walsh G. C., "Optimization of a three DOF translational platform for well-conditioned workspace," 1997, https://doi.org/10.1002/rob.8118 .

[11] Gosselin C. M., "The optimum design of robotic manipulators using dexterity indices," *Robotics and Autonomous Systems,* vol. 9, pp. 213-226, 1992, https://doi.org/10.1016/0921-8890(92)90039-2 .

[12] Aboulissane B., El Bakkali L., and El Bahaoui J., "Workspace analysis and optimization of the parallel robots based on computer-aided design approach," *Facta Universitatis, Series: Mechanical Engineering,* vol. 18, pp. 079-089, 2020, https://doi.org/10.22190/fume190428006a .

[13] Oarcea A., Popister F., Stan S.-D., et al. , "Comparative study of CAD optimization features for the workspace of 3DOF Parallel Robot," in *2021 9th International Conference on Modern Power Systems (MPS)*, 2021, pp. 1-6, https://doi.org/10.1109/mps52805.2021.9492529 .

[14] Laribi M. A., Romdhane L., and Zeghloul S., "Analysis and dimensional synthesis of the DELTA robot for a prescribed workspace," *Mechanism and Machine Theory,* vol. 42, pp. 859-870, 2007, https://doi.org/10.1016/j.mechmachtheory.2006.06.012 .

[15] McCormick E., Wang Y., and Lang H., "Optimization of a 3-RRR Delta robot for a desired workspace with real-time simulation in MATLAB," in *2019 14th International Conference on Computer Science & Education (ICCSE)*, 2019, pp. 935-941, https://doi.org/10.1109/iccse.2019.8845388 .

[16] Zhang L. and Song Y., "Optimal design of the Delta robot based on dynamics," in *2011 IEEE International Conference on Robotics and Automation*, 2011, pp. 336-341, https://doi.org/10.1109/icra.2011.5979731 .

[17] Mirz C., Uzsynski O., Angeles J., et al. , "Stiffness optimization of Delta robots," in *Symposium on Robot Design, Dynamics and Control*, 2020, pp. 396-404, https://doi.org/10.1007/978-3-030-58380-4_48 .

[18] Stock M. and Miller K., "Optimal kinematic design of spatial parallel manipulators: Application to linear delta robot," *Journal of Mechanical Design, Transactions of the ASME,* vol. 125, pp. 292-301, 2003, https://doi.org/10.1115/1.1563632 .

[19] Miller K., "Optimal design and modeling of spatial parallel manipulators," *The International Journal of Robotics Research,* vol. 23, pp. 127-140, 2004, https://doi.org/10.1177/0278364904041322 .

[20] Kelaiaia R., Company O., and Zaatri A., "Multiobjective optimization of a linear Delta parallel robot," *Mechanism and Machine Theory,* vol. 50, pp. 159-178, 2012, https://doi.org/10.1016/j.mechmachtheory.2011.11.004 .

[21] Bounab B., "Multi-objective optimal design based kineto-elastostatic performance for the DELTA parallel mechanism," *Robotica,* vol. 34, pp. 258-273, 2016, https://doi.org/10.1017/s0263574714001416 .

[22] Yang F., Wang L., Chen M., et al. , "Topology and parameterization based multi-objective optimization of Delta parallel robot arm," in *2021 WRC Symposium on Advanced Robotics and Automation (WRC SARA)*, 2021, pp. 212-217, https://doi.org/10.1109/wrcsara53879.2021.9612620 .

[23] Ohno M. and Takeda Y., 2021. Design of target trajectories for the detection of joint clearances in parallel robot based on the actuation torque measurement. Mechanism and Machine Theory, 155, p.104081, 2021, https://doi.org/10.1016/j.mechmachtheory.2020.104081]

[24] Carabin G., Scalera L., Wongratanaphisan T. et al. , 2021. An energy-efficient approach for 3D printing with a linear Delta robot equipped with optimal springs. Robotics and Computer-Integrated Manufacturing, 67, p.102045, 2021, https://doi.org/10.1016/j.rcim.2020.102045 .

[25] Pham Van Bach N., Dam Hai Q., and Bui Trung T., "Optimization of trajectory tracking control of 3-DOF translational robot use PSO method based on inverse dynamics control for surgery application," *Journal of Vibroengineering,* vol. 23, pp. 1591-1601, 2021, https://doi.org/10.21595/jve.2021.21997 .

[26] Falezza, F., Vesentini, F., Di Flumeri, A., et al. , 2022. A novel inverse dynamic model for 3-DoF delta robots. Mechatronics, 83, p.102752, 2022, https://doi.org/10.1016/j.mechatronics.2022.102752 .

[27] Codourey A., "Dynamic modeling of parallel robots for computed-torque control implementation," *The International Journal of Robotics Research,* vol. 17, pp. 1325-1336, 1998, https://doi.org/10.1177/027836499801701205 .

[28] Codourey A., "Dynamic modelling and mass matrix evaluation of the DELTA parallel robot for axes decoupling control," in *Intelligent Robots and Systems' 96, IROS 96, Proceedings of the 1996 IEEE/RSJ International Conference on*, 1996, pp. 1211-1218, https://doi.org/10.1109/iros.1996.568973 .
[29] Codourey A. and Burdet E., "A body-oriented method for finding a linear form of the dynamic equation of fully parallel robots," in *Robotics and Automation, 1997. Proceedings., 1997 IEEE International Conference on*, 1997, pp. 1612-1618, https://doi.org/10.1109/robot.1997.614371 .
[30] Staicu S., "Recursive modelling in dynamics of Delta parallel robot," *Robotica,* vol. 27, pp. 199-207, 2009, https://doi.org/10.1017/s0263574708004451 .
[31] Gholami, A., Homayouni, T., Ehsani, R. et al. , 2021. Inverse kinematic control of a delta robot using neural networks in real-time. Robotics, 10(4), p.115. 2021, https://doi.org/10.3390/robotics10040115]
[32] Boudjedir, C.E. and Boukhetala, D., 2021. Adaptive robust iterative learning control with application to a Delta robot. Proceedings of the Institution of Mechanical Engineers, Part I: Journal of Systems and Control Engineering, 235(2), pp.207-221, 2021, https://doi.org/10.1177/0959651820938531 .
[33] Azad, F.A., Rad, S.A. and Arashpour, M., 2022. Back-stepping control of delta parallel robots with smart dynamic model selection for construction applications. Automation in Construction, 137, p.104211, 2022, https://doi.org/10.1016/j.autcon.2022.104211 .]
[34] Merlet J. P., "Direct kinematics of parallel manipulators," *IEEE Transactions on Robotics and Automation,* vol. 9, pp. 842-846, 1993., https://doi.org/10.1109/70.265928
[35] Gosselin W.-., "A new approach for the dynamic analysis of parallel manipulators," *Kluwer Academic Publishers,* 1998, https://doi.org/10.1115/detc97/dac-3759 .
[36] Fanuc, "M-2iA/3S Fanuc Delta Robot," in *M-2iA*, ed.
[37] Guglielmetti P., "Model-based control of fast parallel robots," EPFL1994, thesis.
[38] Vivas A. and Poignet P., "Predictive functional control of a parallel robot," *Control Engineering Practice,* vol. 13, pp. 863-874, 2005. https://doi.org/10.1016/j.conengprac.2004.10.001
[39] "Maxon Motors - Planetary Gearhead GP 52 C," ed, 2017.
[40] Brans J.-P. and De Smet Y., "PROMETHEE methods," in *Multiple criteria decision analysis*, ed: Springer, 2016, pp. 187-219. https://doi.org/10.1007/978-1-4939-3094-4_6
[41] Greco S., Figueira J., and Ehrgott M., *Multiple criteria decision analysis* vol. 37: Springer, 2016. https://doi.org/10.1007/978-1-4939-3094-4

Figure captions:

Table captions:

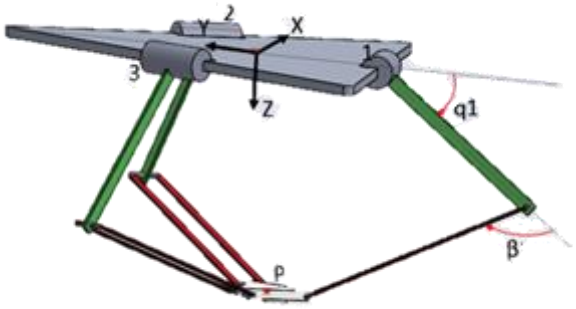

Figure 1. Input angles and output position

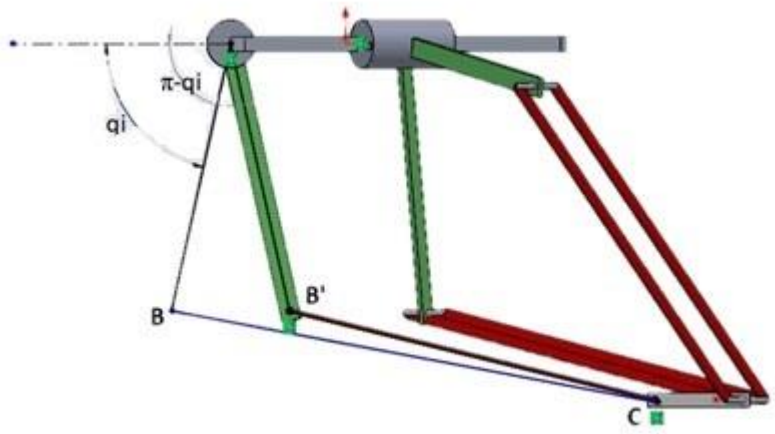

Figure 2. Distinguishing the correct angle between two supplementary angles

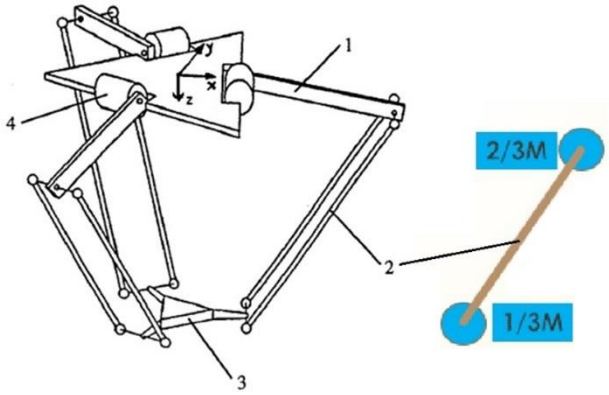

Figure 3. distributing parallelogram's mass [24]

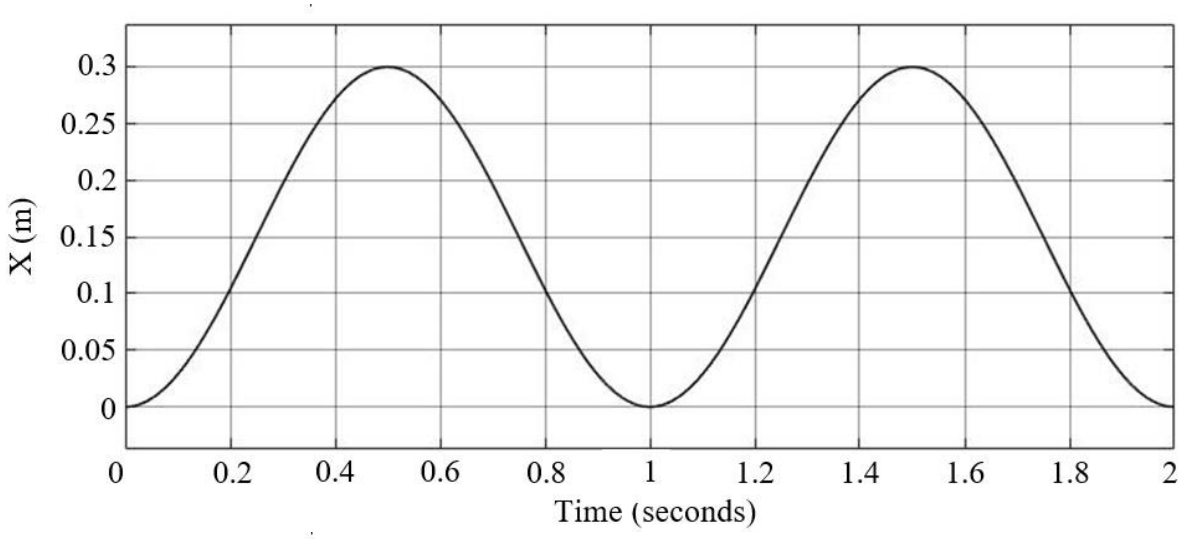

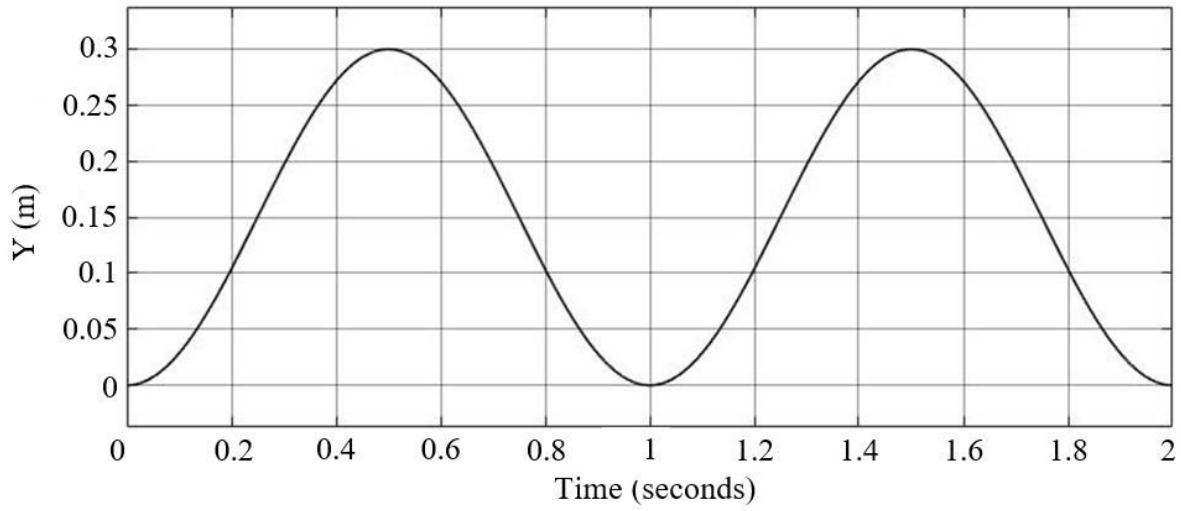

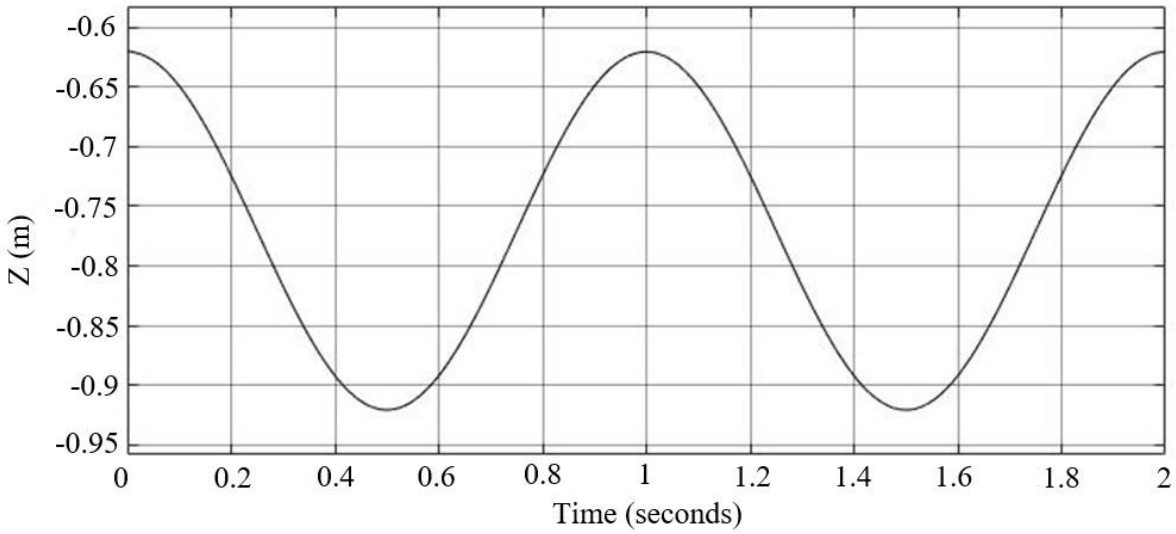

Figure 4. Position-time diagram for the desired path

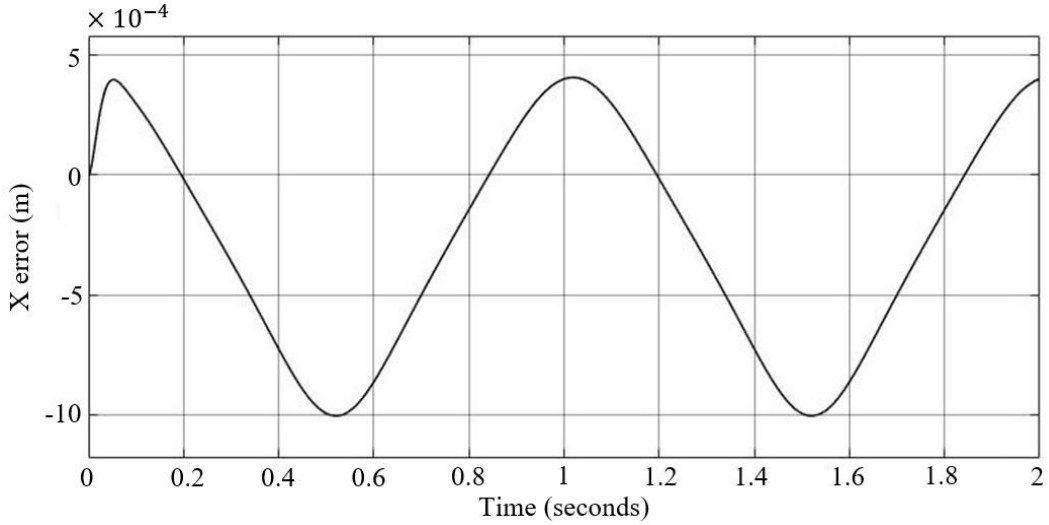

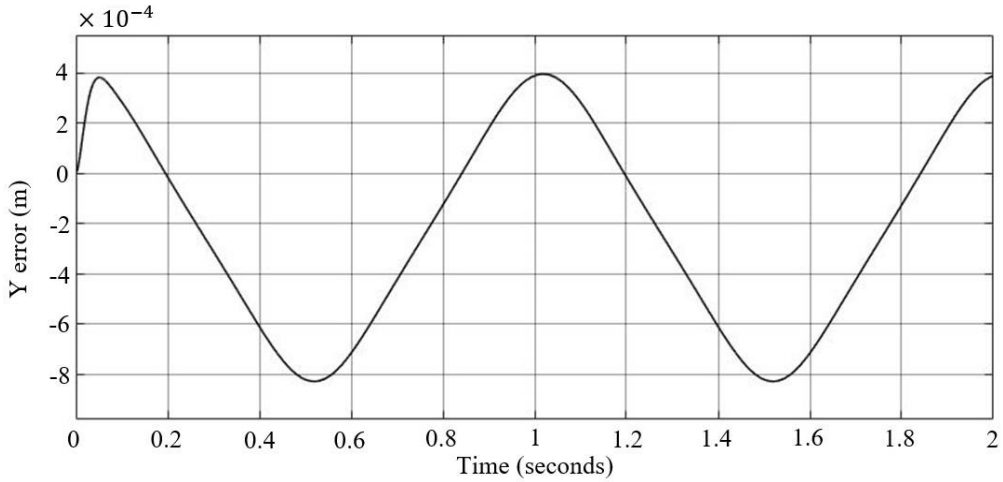

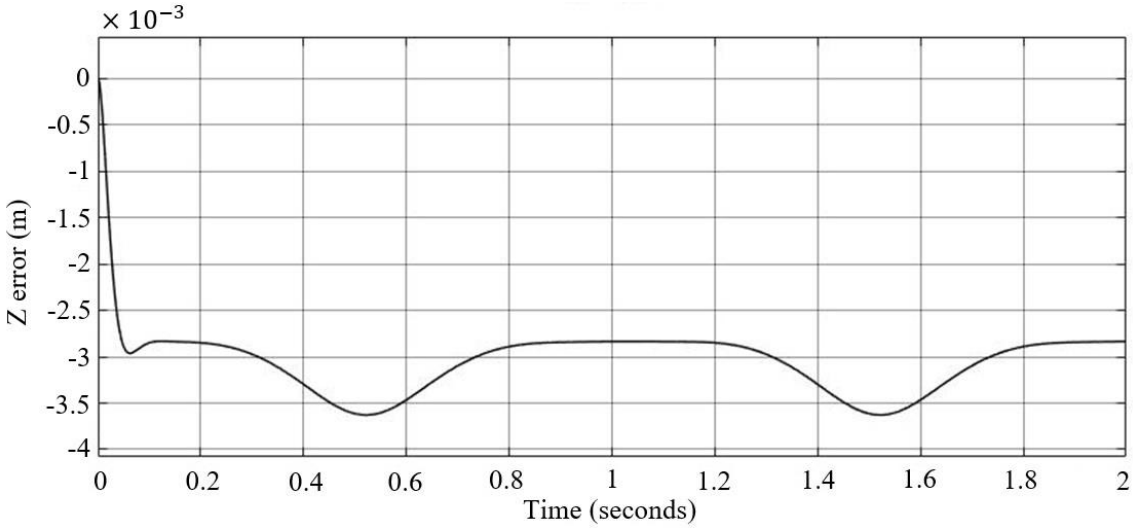

Figure 5. Simplified dynamics error

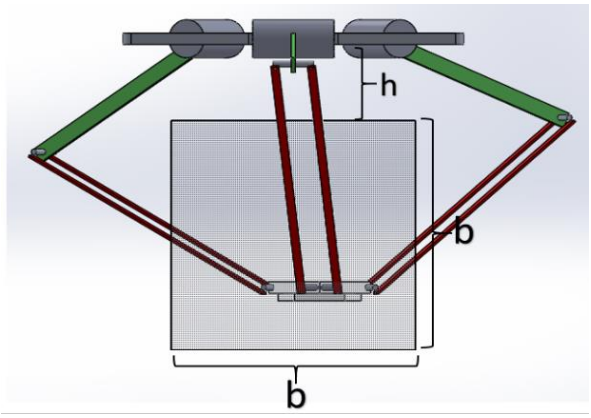

Figure 6. Desired workspace of the Delta Robot

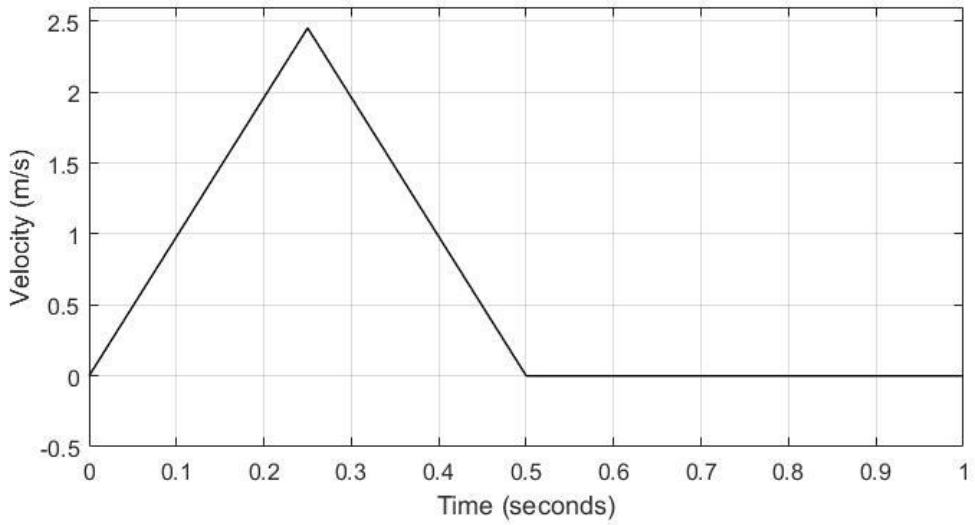

Figure 7. Desired Bang-Bang path velocity-time diagram

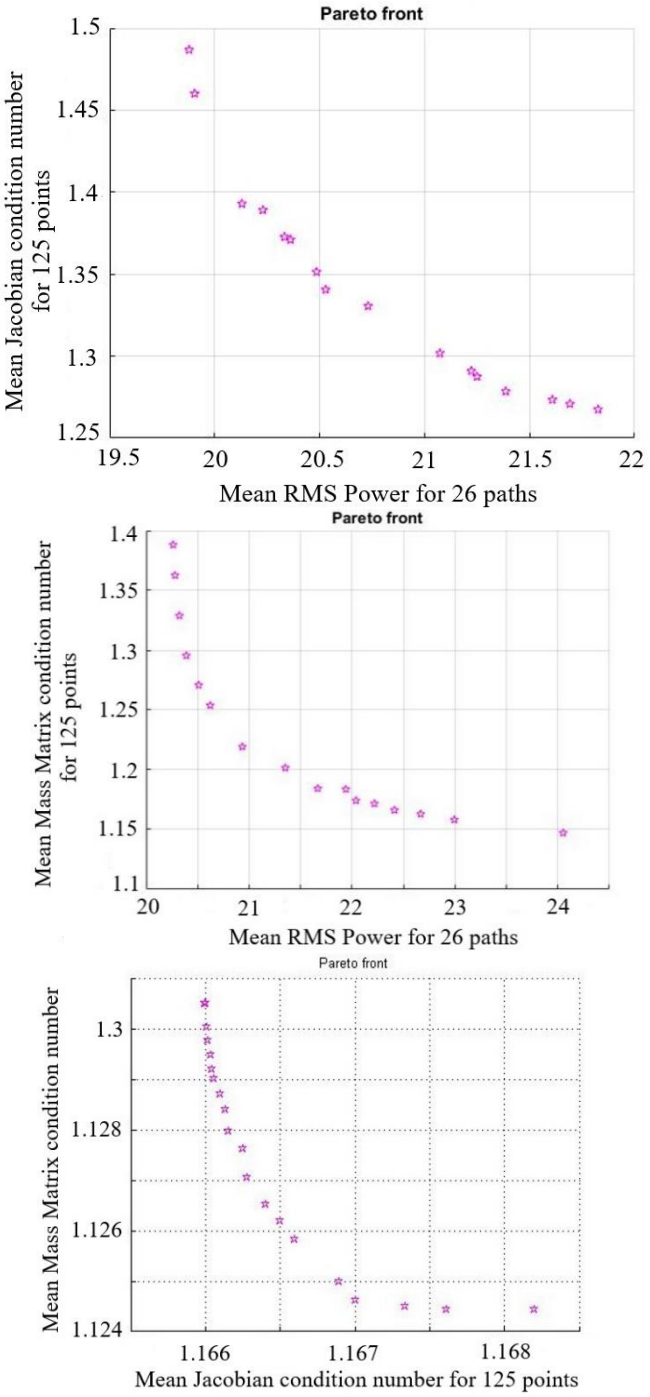

Figure 8. Pareto fronts for two-objective optimizations

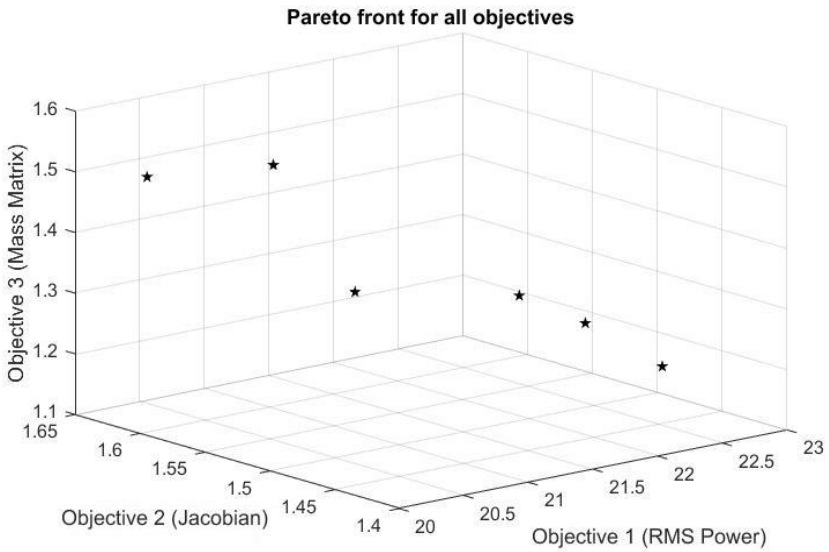

Figure 9. Pareto Surface for three-objective optimization

Table 1. Optimization results for one-objective problem

Objective	L1 (m)	L2 (m)	R (m)	h(m)	Best value
Power RMS	0.632	1	0.162	0.4	17.83 watts
Condition number of Jacobian	0.837	1	0.003	0.385	1.248
Condition number of Mass matrix	0.788	1	0.046	0.499	1.141

Table 2. Dominant answers for the three-objective problem

Criteria			Design parameters			
Power RMS (w)	Jacobian condition number	Mass matrix Condition number	*L1 (m)*	*L2 (m)*	*R (m)*	*h (m)*
21.87	1.4430	1.2981	0.647	0.811	0.016	0.236
21.00	1.5968	1.5009	0.584	0.795	0.101	0.226
22.09	1.5158	1.2887	0.659	0.970	0.235	0.424
21.20	1.5537	1.3098	0.563	0.788	0.103	0.267
22.56	1.4524	1.1911	0.609	0.843	0.094	0.349
20.35	1.6293	1.4891	0.570	0.870	0.149	0.317

Table 3- Normalized decision matrix

Alternative	Power RMS	Jacobian condition number	Mass matrix condition number
A1	0.335	0.478	0.403
A2	0.472	0.355	0.240
A3	0.300	0.410	0.416
A4	0.440	0.382	0.388
A5	0.226	0.468	0.629
A6	0.574	0.336	0.246

Table 4- Alternative ranking based on CODAS method

Alternative	Euclidean	Texicab	Score	Rank
A1	0.090	0.127	-0.119	5
A2	0.074	0.075	-0.212	6
A3	0.092	0.117	-0.103	4
A4	0.099	0.143	-0.063	3
A5	0.197	0.207	0.527	1
A6	0.105	0.108	-0.028	2

Table 5- Rankings resulted from PROMETHEE II method

Alternative	phi+	phi-	phi	Rank
A1	0.060	0.077	-0.017	3
A2	0.044	0.171	-0.127	6
A3	0.059	0.089	-0.030	4
A4	0.071	0.059	0.012	2
A5	0.310	0.090	0.220	1
A6	0.104	0.162	-0.058	5

Table 6- Rankings based on ELECTRE method

Alternative	Concordance	Discordance	Score	Rank
A1	0.492	-0.013	0.505	3
A2	-1.528	2.842	-4.370	6
A3	0.356	1.168	-0.812	5
A4	-0.172	-1.537	1.365	2
A5	0.700	-2.342	3.042	1
A6	0.152	-0.118	0.270	4

Table 7. Comparison of the results with an industrial robot

		Designed	Fanuc M-2iA/3S [29]
Design Variables	L1 (m)	0.609	0.32
	L2 (m)	0.843	0.681
	R (m)	0.094	0.02
	h (m)	0.349	0.386
	L1 / L2	0.722	0.470
Fitness Functions	Power RMS (W)	22.56	29.05
	Average Jacobian condition No.	1.4524	4.0564
	Maximum Jacobian condition No.	2.1912	18.6475
	Average mass matrix condition No.	1.1911	1.6268
	Maximum mass matrix condition No.	1.6295	4.3575

Yussuf Reza Esmaeili received the B.Sc. and M.Sc. degrees in Mechanical Engineering from the Sharif University of Technology in 2016 and 2018, respectively. He is currently pursuing the Ph.D. degree with the Department of Mechanical Engineering, University of Victoria, Canada. His current research interests include advanced system and automation and machine learning.

Hamed Moradi received the B.Sc., Mechanical Engineering degree in solid mechanics from Amirkabir University of Technology (Tehran Polytechnic) in 2005; M.Sc. & PhD Mech. Eng. in applied mechanics from Sharif University of Technology (SUT), Tehran, Iran in 2008 and 2012. Currently, he is the Associate Professor in the Department of Mechanical Engineering, Sharif University of Technology. His current research interests include the modeling of dynamic systems, application of robust, nonlinear and optimal control methods in various dynamics systems such as manufacturing, bio-engineering, thermo-fluid industrial processes, renewable energy and power plant engineering

Gholamreza Vossoughi received his Ph.D. from Mechanical Engineering Dept. at University of Minnesota in 1992. Ever since he has been a faculty member of Mechanical Engineering Dept. at Sharif University of Technology. He has served as the Manufacturing Engineering and Applied Mechanics Division Directors from 1994 to 1998 and as the Graduate Dean of the Mechanical Engineering from 1999-2003. Currently, he is the Professor in the Department of Mechanical Engineering, Sharif University of Technology.